Reinforcement Learning with Latent Flow

Wenling Shang[*]
DeepMind
wendyshang@deepmind.com

Xiaofei Wang[*]
UC Berkeley
w.xf@berkeley.edu

Aravind Srinivas
OpenAI
aravind_srinivas@berkeley.edu

Aravind Rajeswaran
Facebook AI Research, University of Washington
aravraj@fb.com

Yang Gao
Tsinghua University
gaoyangiiis@tsinghua.edu.cn

Pieter Abbeel
UC Berkeley, Covariant
pabbeel@berkeley.edu

Michael Laskin
UC Berkeley
mlaskin@berkeley.edu

Abstract

Temporal information is essential to learning effective policies with Reinforcement Learning (RL). However, current state-of-the-art RL algorithms either assume that such information is given as part of the state space or, when learning from pixels, use the simple heuristic of frame-stacking to implicitly capture temporal information present in the image observations. This heuristic is in contrast to the current paradigm in video classification architectures, which utilize explicit encodings of temporal information through methods such as optical flow and two-stream architectures to achieve state-of-the-art performance. Inspired by leading video classification architectures, we introduce the **F**low of **La**tents for **Re**inforcement Learning (*Flare*), a network architecture for RL that explicitly encodes temporal information through latent vector differences. We show that Flare recovers optimal performance in state-based RL without explicit access to the state velocity, solely with positional state information. Flare is the most sample efficient model-free pixel-based RL algorithm on the DeepMind Control suite when evaluated on the 500k and 1M step benchmarks across 5 challenging control tasks, and, when used with Rainbow DQN, outperforms the competitive baseline on Atari games at 100M time step benchmark across 8 challenging games.

1 Introduction

Reinforcement learning (RL) [41] holds the promise of enabling artificial agents to solve a diverse set of tasks in uncertain and unstructured environments. Recent developments in RL with deep neural networks have led to tremendous advances in autonomous decision making. Notable examples include classical board games [36, 37], video games [29, 6, 45], and continuous control [34, 28]. There has been a large body of research on extracting high quality features during the RL process, such as with auxiliary losses [20, 27, 35] or data augmentation [25, 26]. However, another important component in RL representation learning has been largely overlooked: a more effective architecture to incorporate temporal features. This becomes especially crucial in an unstructured real-world setup like the home when compact state representations such as calibrated sensory inputs are unavailable. Motivated by this understanding, we explore architectural improvements to better utilize temporal features for the problem of efficient and effective deep RL from pixels.

[*]Equal contribution

35th Conference on Neural Information Processing Systems (NeurIPS 2021).

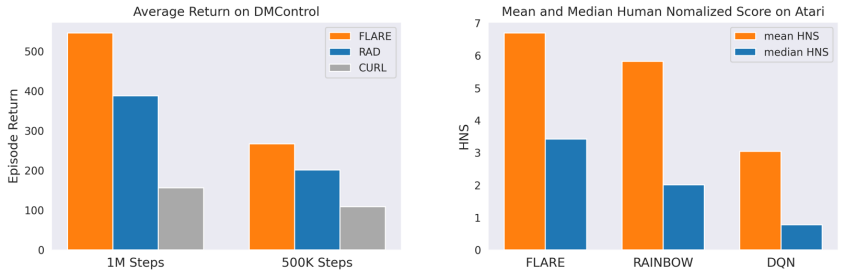

Figure 1: Mean and median evaluation scores on DMControl[42] and Atari[3]. Flare is an architectural modification that improves RAD and Rainbow, the base algorithms it integrates with.

Current approaches in deep RL for learning temporal features are largely heuristic in nature. A commonly employed approach is to stack the most recent frames [29] as inputs to a convolutional neural network (CNN). This can be interpreted as a form of early fusion [24], where information from the recent time window is combined at the pixel level for input to the CNN. In contrast, modern video recognition systems use alternate architectures that employ optical flow and late fusion [38], where frames are processed individually with CNN layers before fusion and downstream processing. Late fusion is typically beneficial due to better performance, fewer parameters, and the ability to use multi-modal data [8, 21]. However, it is not straightforward how to directly extend such architectures to RL. Real-time computation of optical flow for action selection can be computationally infeasible for many applications with fast control loops like robotics. Furthermore, optical flow computation at training time can also be prohibitively expensive. In our experiments, we also observe that a naive late fusion architecture minus the optical flow yields poor results in RL settings (see Section 6.3). This observation is consistent with recent findings in related domains like visual navigation [46].

To overcome the above challenges, we develop **F**low of **La**tents for **Re**inforcement Learning (*Flare*), a new architecture for deep RL from pixels (Figure 4). Flare can be interpreted as a *structured late fusion* architecture. It processes each frame individually to compute latent vectors, similar to a standard late fusion approach. Subsequently, temporal differences between the latent feature vectors are computed and fused along with the latent vectors by concatenation for downstream processing. By incorporating this structure of temporal difference in latent feature space, we provide the learning agent with appropriate inductive bias.

We highlight the main empirical contributions from Flare in the following[2]:

1. Flare recovers optimal performance in state-based RL without explicit access to the state velocity, solely with positional state information.
2. Flare achieves state-of-the-art performance compared to model-free methods on several *challenging* pixel-based continuous control tasks within the DeepMind control benchmark suite [42], while being the most sample efficient model-free pixel-based RL algorithm across these tasks, outperforming the prior model-free state-of-the-art RAD on the 500k and 1M environment step benchmarks respectively (Figure 1). A video demonstration of Flare achieving SOTA performance on Quadruped Walk is in the supplementary materials.
3. When augmented over Rainbow DQN, Flare outperforms the baseline on 5 out of 8 challenging Atari games at 100M step benchmark. Notebly, Flare scores 1668 on Montezuma's Revenge, a signifcant gain over the baseline Rainbow DQN's 900.

2 Related Work

Pixel-Based RL The ability of an agent to autonomously learn control policies from visual inputs can greatly expand the applicability of deep RL [10, 32]. Prior works have used CNNs to extend RL algorithms like PPO [34], SAC [14], and Rainbow [19] to pixel-based tasks. Such direct extensions have typically required substantially larger number of environment interactions when compared to the state-based environments. In order to improve sample efficiency, recent efforts have studied the use of auxiliary tasks and loss functions [50, 27, 35], data augmentation [26, 25], and latent space

[2]Code: https://github.com/WendyShang/flare

dynamics modeling [16, 15]. Despite these advances, there is still a large gap between the learning efficiency in state-based and pixel-based environments in a number of challenging benchmark tasks. Our goal in this work is to identify where and how to improve pixel-based performance on this set of challenging control environments.

Neural Network Architectures in RL Mnih et al. [29] combined Q-learning with CNNs to achieve human level performance in Atari games, wherein Mnih et al. [29] concatenate the most recent 4 frames and use a convolutional neural network to output the Q values. In 2016, Mnih et al. [30] proposed to use a shared CNN among frames to extract visual features and aggregate the temporal information with LSTM. The same architectures have been adopted by most works to date [27, 35, 25, 26]. Recently, new architectures for RL have been explored that explore dense connections [39] as well as residual connections and instance norm [49]. However, the development of new architectures to better capture temporal information in a stream of images has received little attention in deep RL, and our work fills this void. Perhaps the closest to our motivation is the work of Amiranashvili et al. [1] who explicitly use optical flow as an extra input to the RL policy. However, this approach requires additional information and supervision signal to train the flow estimator, which could be unavailable or inaccurate in practice. In contrast, our approach is a simple modification to existing deep RL architectures and does not require any additional auxiliary tasks or supervision signals.

Two-Stream Video Classification In video classification tasks, such as activity recognition [40], there are a large body of works on how to utilize temporal information [9, 22, 44, 7, 47, 12]. Of particular relevance is the two-stream architecture of Simonyan and Zisserman [38], where one CNN stream takes the usual RGB frames, while the other the optical flow computed from the RGB values. The features from both streams are then late-fused to predict the activity class. That the two-stream architecture yields a significant performance gain compared to the single RGB stream counterpart, indicating the explicit temporal information carried by the flow plays an essential role in video understanding. Instead of directly computing the optical flow, we propose to capture the motion information in latent space to avoid computational overheads and potential flow approximation errors. Our approach also could focus on domain-specific motions that might be overlooked in a generic optical flow representation.

3 Background

Soft Actor Critic (SAC) [14] is an off-policy actor-critic RL algorithm for continuous control with an entropy maximization term augmented to its score function to encourage exploration. SAC learns a policy network $\pi_\psi(a_t|\mathbf{o}_t)$ and critic networks $Q_{\phi_1}(\mathbf{o}_t, a_t)$ and $Q_{\phi_2}(\mathbf{o}_t, a_t)$ to estimate state-action values. The critic $Q_{\phi_i}(\mathbf{o}_t, a_t)$ is optimized to minimize the (soft) Bellman residual error:

$$\mathcal{L}_Q(\phi_i) = \mathbb{E}_{\tau\sim\mathcal{B}}\left[\left(Q_{\phi_i}(\mathbf{o}_t, a_t) - (r_t + \gamma V(\mathbf{o}_{t+1}))\right)^2\right],$$

where r is the reward, γ the discount factor, $\tau = (\mathbf{o}_t, a_t, \mathbf{o}_{t+1}, r_t)$ is a transition sampled from replay buffer $\mathcal{B}$, and $V(\mathbf{o}_{t+1})$ is the (soft) target value estimated by:

$$V(\mathbf{o}_{t+1}) = \min_i Q_{\bar{\phi}_i}(\mathbf{o}_{t+1}, a_{t+1}) - \alpha \log \pi_\psi(a_{t+1}|\mathbf{o}_{t+1})],$$

where α is the entropy maximization coefficient. For stability, $Q_{\bar{\phi}_i}$ is the exponential moving average of Q_{ϕ_i}'s over training iterations. The policy π_ψ is trained to maximize the expected return estimated by Q together with the entropy term

$$L_\pi(\psi) = -\mathbb{E}_{a_t\sim\pi}\left[\min_i Q_{\phi_i}(\mathbf{o}_t, a_t) - \alpha \log \pi_\psi(a_t|\mathbf{o}_t)\right],$$

where α is also a learnable parameter.

Reinforcement Learning with Augmented Data, or RAD [26], is a recently proposed training technique. In short, RAD pre-processes raw pixel observations by applying random data augmentations, such as random translation or cropping, for RL training. As simple as it is, RAD has taken many existing RL algorithms, including SAC, to the next level. For example, on many DMControl [42] benchmarks, while vanilla pixel-based SAC performs poorly, RAD-SAC—i.e. applying data augmentation to pixel-based SAC—achieves state-of-the-art results both in sample efficiency and final performance. In this work, we refer RAD to RAD-SAC and use random translation as data augmentation.

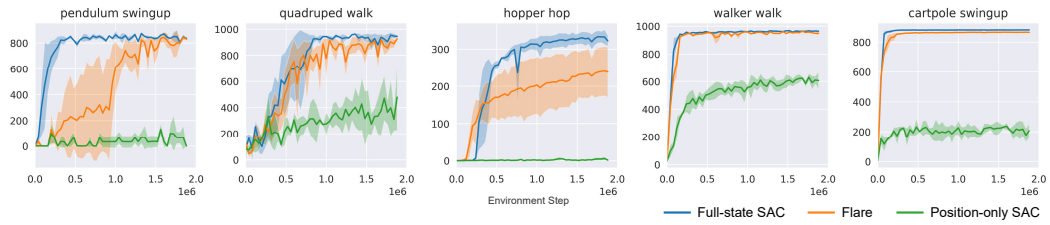

Figure 2: Flare enables an RL agent with only access to positional state to recover a near-optimal policy relative to RL with access to the full state. In the above learning curves we show test-time performance for (i) full-state SAC (blue), where both pose and temporal information is given (ii) position-only SAC (green), and (iii) state-based Flare (orange), where only pose information is provided and velocities are approximated through pose offsets. Unlike full-state SAC, which learns the optimal policy, position-only SAC either fails or converges at suboptimal policies. Meanwhile, the fusion of positions and approximated velocities in Flare efficiently recovers near-optimal policies in most cases. This motivates using Flare for pixel-based input, where velocities are not present in the observation. These results show mean performance with standard deviations averaged over 3 seeds.

Rainbow DQN is an extension of the Deep Q Network (DQN) [29], which combines multiple follow-up improvements of DQN to a single algorithm [19]. In summary, DQN [29] is an off-policy RL algorithm that leverages deep neural networks (DNN) to estimate the Q value directly from the pixel space. The follow-up works Rainbow DQN bring together to enhance the original DQN include double Q learning [17], prioritized experience replay [33], dueling network [48], noisy network [13], distributional RL [5] and multi-step returns [41]. Rainbow DQN is one of the state-of-the-art RL algorithms on the Atari 2600 benchmark [3]. We thus adopt an official implementation of Rainbow [31] as our baseline to directly augment Flare on top.

4 Motivation

We motivate Flare by investigating the importance of temporal information in state-based RL. Our investigation utilizes 5 diverse DMControl [42] tasks. The full state for these environments includes both the agent's pose information, such as the joints' positions and angles, as well as temporal information, such as the joints' translational and angular velocities.

First, we train two variants with SAC—one where the agent receives the full state as input (full-state SAC), and the other with the temporal information masked out, i.e. the agent only receives the pose information as its input (position-only SAC). The resulting learning curves are in Figure 2. While the full-state SAC learns the optimal policy quickly, the position-only SAC learns much sub-optimal policies, which often fail entirely. Therefore, we conclude that effective policies cannot be learned from positions alone, and that temporal information is crucial for efficient learning.

While full-state SAC can receive velocity information from internal sensors in simulation, in the more general case such as learning from pixels, such information is often not readily available. For this reason, we attempt to approximate temporal information as the difference between two consecutive states' positions. Concretely, we compute the positional offset $\delta_t = (s^p_t - s^p_{t-1}, s^p_{t-1} - s^p_{t-2}, s^p_{t-2} - s^p_{t-3})$, and provide the fused vector (s^p_t, δ_t) to the SAC agent. This procedure describes the state-based version of Flare. Results shown in Figure 2 demonstrate that state-based Flare significantly outperforms the position-only SAC. Furthermore, it achieves optimal asymptotic performance and a learning efficiency comparable to full-state SAC in most environments.

Given that the position-only SAC utilizes s^p_t compared to Flare that utilizes s^p_t and δ_t, we also investigate a variant (stack SAC) where the SAC agent takes consecutive positions $(s^p_t, s^p_{t-1}, s^p_{t-2}, s^p_{t-3})$. Stack SAC reflects the frame-stack heuristic used in pixel-based RL. Results in Figure 3 show that Flare still significantly outperforms stack SAC. It suggests that the well-structured inductive bias in the form of temporal-position fusion is essential for efficient learning.

Lastly, since a recurrent structure is an alternative approach to process temporal information, we implement an SAC variant with recurrent modules (Recurrent SAC) to compare with Flare. Specifically,

we pass a sequence of poses $s^p_t, s^p_{t-1}, s^p_{t-2}, s^p_{t-3}$ through an LSTM cell. The number of the LSTM hidden units h is set to be the same as the dimension of δ_t in Flare. The trainable parameters of the LSTM cell are updated to minimize the critic loss. Recurrent SAC is more complex to implement and requires longer wall-clock training time, but performs worse than Flare as shown in Figure 3.

Our findings from the state experiments in Figure 2 and Figure 3 suggest that (i) temporal information is crucial to learning effective policies in RL, (ii) using Flare to approximate temporal information in the absence of sensors that provide explicit measurements is sufficient in most cases, and (iii) to incorporate temporal information via naively staking position states or a recurrent module are less effective than Flare. In the next section, we carry over these insights to pixel-space RL.

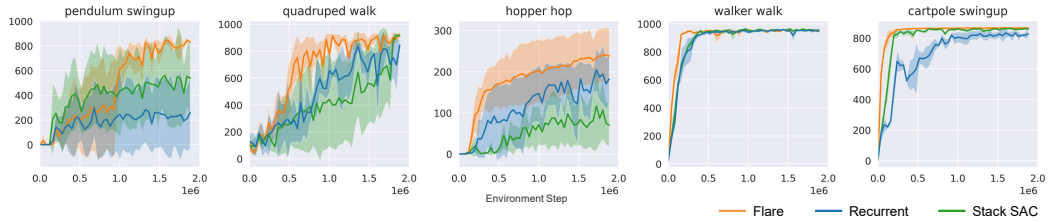

Figure 3: We compare 3 ways to incorporate temporal information: i) Flare (orange) receives $(s^p_t, s^p_t - s^p_{t-1}, s^p_{t-1} - s^p_{t-2}, s^p_{t-2} - s^p_{t-3})$, ii) stack SAC (green) stacks $(s^p_t, s^p_{t-1}, s^p_{t-2}, s^p_{t-3})$ as inputs, and iii) recurrent SAC (blue) uses recurrent layers to process $(s^p_t, s^p_{t-1}, s^p_{t-2}, s^p_{t-3})$. Stack SAC and recurrent SAC perform significantly worse than Flare on most environments, highlighting the benefit of how Flare handles temporal information. Results are averaged over 3 seeds.

5 Reinforcement Learning with Latent Flow

To date, frame stacking is the most common way of pre-processing pixel-based input to convey temporal information for RL algorithms. This heuristic, introduced by Mnih et al. [29], has been largely untouched since its inception and is used in most state-of-the-art RL architectures. However, our observations from the experiments run on state inputs in Section 4 suggest an alternative to the frame stacking heuristic through the explicit inclusion of temporal information as part of the input. Following this insight, we seek a general alternative approach to explicitly incorporate temporal information that can be coupled to any base RL algorithm with minimal modification. To this end, we propose the **F**low of **La**tents for **Re**inforcement Learning (*Flare*) architecture. Our proposed method calculates differences between the latent encodings of individual frames and fuses the feature differences and latent embeddings before passing them as input to the base RL algorithm, as shown in Figure 4. We demonstrate Flare on top of 2 state-of-the-art model-free off-policy RL baselines, RAD-SAC [26] and Rainbow DQN [19], though in principle any RL algorithm can be used in principle.

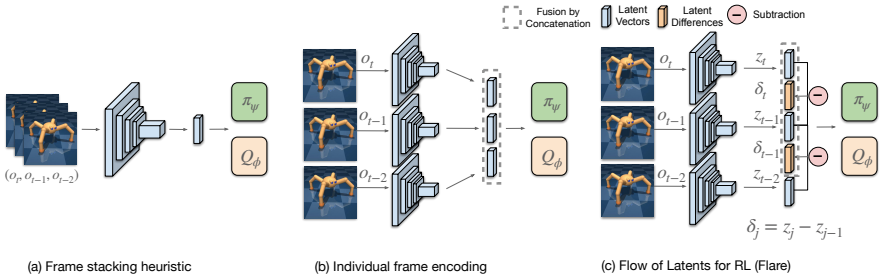

Figure 4: **F**low of **La**tents for **Re**inforcement Learning (*Flare*): (a) the architecture for the frame stacking heuristic, (b) an alternative to the frame stacking hueristic by encoding each image individually, and (c) the Flare architecture which encodes images individually, computes the feature differences, and fuses the differences together with the latents.

5.1 Latent Flow

In computer vision, the most common way to explicitly inject temporal information of a video sequence is to compute dense optical flow between consecutive frames [38]. Then the RGB and the optical flow inputs are individually fed into two streams of encoders and the features from both are fused in the later stage of the pipelinee. But two-stream architectures with optical flow are not as applicable to RL, because it is too computationally costly to generate optical flow on the fly.

To address this challenge and motivated by experiments in Section 4, we propose an alternative architecture that is similar in spirit to the two-stream networks for video classification. Rather than computing optical flow directly, we approximate temporal information in the latent space. Instead of encoding a stack of frames at once, we use a frame-wise CNN to encode each individual frame. Then we compute the differences between the latent encodings of consecutive frames, which we refer to as *latent flow*. Finally, the latent features and the latent flow are fused together through concatenation before getting passed to the downstream RL algorithm. We call the proposed architecture as **F**low of **La**tents for **Re**inforcement Learning (*Flare*).

5.2 Implementation and Architecture Details

Algorithm 1 Pixel-based Flare Inference

Given π_ψ, f_{CNN}
for each environment step t **do**
  $z_j{=}f_{\text{CNN}}(o_j), j{=}t{-}k, .., t$
  $\delta_j{=}z_j{-}z_{j-1}, j{=}t{-}k{+}1, .., t$
  $\mathbf{z}_t{=}(z_{t-k+1}, \cdots, z_t, \delta_{t-k+1}, \cdots, \delta_t)$
  $\mathbf{z_t} = \text{LayerNorm}(f_{\text{FC}}(\mathbf{z_t}))$
  $a_t{\sim}\pi_\psi(a_t|\mathbf{z}_t)$
  $o_{t+1}{\sim}p(o_{t+1}|a_t, \mathbf{o}_t = (o_t, o_{t-1}..o_{t-k}))$

We select RAD as the base algorithm to elaborate the execution of Flare. Similar adaptations can be seamlessly applied to other RL algorithms such as Rainbow DQN. The RAD architecture, shown in Figure 4a, stacks multiple data augmented frames observed in the pixel space and encodes them altogether through an CNN. This can be viewed as a form of early fusion [24].

Another preprocessing option is to encode each frame individually through a shared frame-wise encoder and perform late fusion of the resulting latent features, as shown in Figure 4b. However, we find that simply concatenating the latent features results in inferior performance when compared to the frame stacking heuristic, which we further elaborate in Section 6.3. We conjecture that pixel-level frame stacking benefits from leveraging both the CNN and the fully connected layers to process temporal information, whereas latent-level stacking does not propagate temporal information back through the CNN encoder.

Based on this conjecture, we explicitly compute the latent flow $\delta_t = z_t - z_{t-1}$ while detaching the z_{t-1} gradients when computing δ_t. We then fuse together (δ_t, z_t). Next, since negative values in the fused latent embedding now possesses semantic meaning from δ_t, instead of ReLU non-linearity, we pass the embedding through a fully-connected layer followed by layer normalization, before entering the actor and critic networks as shown in Figure 4c. Pseudocode illustrates inference with Flare in Algorithm 5.2; during training, the encodings of latent features and flow are done in the same way except with augmented observations.

6 Experiments

In this section, we first present the main experimental results, where we show that Flare achieves substantial performance gains over the base algorithm RAD [26] and Rainbow DQN [19]. Then we conduct a series of ablation studies to stress test the design choices of the Flare architecture.

6.1 Environments and Evaluation Metrics

The DeepMind Control Suite (DMControl) [42], based on MuJoCo [43], is a commonly used benchmark for continuous control from pixels. On simpler environments in the suite, prior works [25, 26] have made substantial progress on this benchmark and closed the gap between state-based and pixel-based efficiency. However, on more challenging environments that feature partial observability, sparse rewards, or precise manipulation, these algorithms struggle to learn optimal policies efficiently . In this work, we focus on 5 of these more challenging tasks. The 5 environments include Walker

Table 1: Mean returns and standard errors on 5 challenging DMControl tasks evaluated at 500K and 1M environment steps over 5 random seeds and 10 trajectories per seed. Flare substantially outperforms RAD on a majority (3 out of the 5) of environments, while remaining competitive in the remaining ones and achieving a substantially higher aggregate scores.

	1M STEPS			500K STEPS		
TASK	FLARE	RAD	CURL	FLARE	RAD	CURL
QUADRUPED WALK	**488** $\pm$ 99	322 $\pm$ 102	38 $\pm$ 10	**296** $\pm$ 62	206 $\pm$ 50	39 $\pm$ 22
PENDULUM SWINGUP	**809** $\pm$ 14	520 $\pm$ 144	151 $\pm$ 48	**242** $\pm$ 68	79 $\pm$ 33	46 $\pm$ 207
HOPPER HOP	**217** $\pm$ 26	211 $\pm$ 12	44 $\pm$ 3	**90** $\pm$ 25	40 $\pm$ 18	10 $\pm$ 17
FINGER TURN HARD	**661** $\pm$ 141	249 $\pm$ 44	222 $\pm$ 14	**282** $\pm$ 30	137 $\pm$ 44	207 $\pm$ 32
WALKER RUN	556 $\pm$ 42	**628** $\pm$ 17	323 $\pm$ 35	426 $\pm$ 18	**547** $\pm$ 21	245 $\pm$ 32
AVERAGE RETURN	**546**	388	156	**267**	202	109

Table 2: Due to large computational requirements for 100M Atari runs, we randomly select 8 Atari games for evaluation. We run 5 random seeds for both Flare and Rainbow DQN [19], evaluate scores at 100m training steps, and show the mean and standard error. Flare improves the Rainbow DQN in most games and achieves a subtantially higher mean and median human normalized scores (HNS). † refers to a comparison being made between Flare and Flare's base algorithm Rainbow. Reference values for DQN, Random, and Human baselines are taken from Bellemare et al. [4].

TASK	FLARE	RAINBOW	DQN	RANDOM	HUMAN
DEFENDER	**86982**$\pm$13065	44694$\pm$1782	23633	2874.5	18688.9
PHOENIX	**60974**$\pm$8070	16992$\pm$1474	8485.2	761.4	7242.6
BERZERK	**2049**$\pm$188	1636$\pm$267	585.6	123.7	2630.4
MONTEZUMA	**1668**$\pm$472	900$\pm$161	0	0	4753.3
ASSAULT	12724$\pm$221	**15229**$\pm$1611	4280.5	222.4	742
BREAKOUT	**345**$^\dagger\pm$10	280$\pm$8	**385.5**	1.7	30.5
SEAQUEST	13901$\pm$3616	**24090**$\pm$5579	5860.6	68.4	42054.7
TUTANKHAM	**248**$\pm$9	**247**$\pm$5	68.1	11.4	167.6
MEDIAN HNS	**3.4**	2.0	0.8	0.0	1.0
AVERAGE HNS	**6.7**	5.8	3.0	0.0	1.0

Run (requires maintaining balance with speed), Quadruped Walk (partially observable agent morphology), Hopper Hop (locomotion with sparse rewards), Finger Turn-hard (precise manipulation), and Pendulum Swingup (torque control with sparse rewards). For evaluation, we benchmark performance at 500K and 1M *environment steps* and compare against RAD.

The Atari 2600 Games [3] is another highly popular RL benchmark. Recent efforts have led to a range of highly successful algorithms [11, 19, 23, 15, 2] to solve Atari games directly from pixel. A representative state-of-the-art is Rainbow DQN (see Section 3). We adopt the official Rainbow DQN implementation [31] as our baseline and simply incorporate Flare while retaining all the other default settings, including hyperparameters and preprocessing. Note that the baseline Rainbow DQN's model architecture is also modified to the most comparable setup to that of Flare as described in Section 5.2, including increasing the number of last layer convolutional channels (to match the number of parameters) and adding a fully-connected layer plus layer normalization before the Q networks. We evaluate on a diverse subset of Atari games at 100M *training steps*, namely Assault, Breakout, Freeway, Krull, Montezuma Revenge, Seaquest, Up n Down and Tutankham, to assess the effectiveness of Flare.

Evaluation and Training Protocol It is a common symptom in RL that evaluations appear noisy. To ensure the most fair presentation of results, we follow this protocol: the main results in Section 6.2 report the mean over 5 random seeds with standard error, a standard RL practice [42, 31]. Furthermore, we use the same 5 seeds for both the baseline and Flare.

6.2 Main Results

We present the main results of comparing Flare against the baselines, namely RAD and Rainbow DQN. Flare outperforms the baselines on the majority of the environments. It is worth noting that since these baselines already produce state-of-the-art level performances, any steady improvement under our rigorous experimental protocol—even when the gain seems minor —is significant.

DMControl: Our main experimental results on the 5 DMControl tasks are presented in Table 1. We find that Flare outperforms RAD in terms of both final performance and sample efficiency for majority (3 out of 5) of the environments, while being competitive on the remaining environments. Specifically, Flare attains similar asymptotic performance to state-based RL on Pendulum Swingup, Hopper Hop, and Finger Turn-hard. For Quadruped Walk, a particularly challenging environment due to its large action space and partial observability, Flare learns much more efficiently than RAD and achieves a higher final score. Moreover, Flare outperforms RAD in terms of sample efficiency on all of the core tasks except for Walker Run. The 500k and 1M environment step evaluations in Table 1 show that, on average, Flare achieves $\mathbf{1.4}\times$ and $\mathbf{1.3}\times$ higher scores than RAD at the 1M step and the 500K step benchmarks, respectively.

Atari: The results on the 8 Atari games are in Table 2. Again, we observe substantial performance gain from Flare on the majority (5 out of 8) of the games, including the challenging Montezuma's Revenge. On most of the remaining games, Flare is equally competitive except for Seaquest. In the appendix, we also show that Flare performs competitively when comparing against other DQN variants at 100M training steps, including the original Rainbow implementations.

6.3 Ablation Studies

We ablate a number of components of the Flare architecture on the Quadruped Walk and Pendulum Swingup environments to stress test the Flare architecture. The results shown in Figure 5 aim to answer the following questions:

Q1: *Do we need latent flow or is computing pixel differences sufficient?*
A1: Flare proposes a late fusion of latent differences with the latent embeddings, while a simpler approach is an early fusion of pixel differences with the pixel input, which we call pixel flow. We compare Flare to pixel flow in Figure 5 (left) and find that pixel flow is above RAD but significantly less efficient and less stable than Flare, particularly on Quadruped Walk. This ablation suggests that late fusion temporal information after encoding the image is preferred to early fusion.

Q2: *Are the gains coming from latent flow or individual frame-wise encoding?*
A2: We address the potential concern that the performance gain of Flare stems from the frame-wise ConvNet architectural modification instead of the fusion of latent flow. Concretely, we follow the exact architecture and training as Flare, but instead of concatenating the latent flow, we concatenate each frame's latent vector after the convolution encoders directly as described in Figure 4b. This ablation is similar in spirit to the state-based experiments in Figure 3. The learning curves in Figure 5 (center) show that individual frame-wise encoding is not the source of the performance lift: frame-wise encoding, though on par with RAD on Pendulum Swingup, performs significantly worse on Quadruped Walk. Flare's improvements over RAD are hence most likely thanks to the explicit fusion of latent flow.

Q3: *How does the input frame count affect performance?*
A3: We compare stacking 2, 3, and 5 frames in Flare in Figure 5 (right). We find that changing the number of stacked frames does not significantly impact the locomotion task, quadruped walk, but Pendulum Swingup tends to be more sensitive to this hyperparameter. Interestingly, the optimal number of frames for Pendulum Swingup is 2, and more frames can in fact degrade Flare's performance, indicating the immediate position and velocity information is the most critical to learn effective policies on this task. We hypothesize that Flare trains more slowly with increased frame count on Pendulum Swingup due to the presence of unnecessary information that the actor and critic networks need to learn to ignore.

Q4: *Do we need latent flow or is RNN over latent sufficient?*
A4: Another approach of latent fusion would be applying a recurrent neural network on the latent embeddings. We compare FLARE with LSTM baselines on DMControl. We found that RNNs

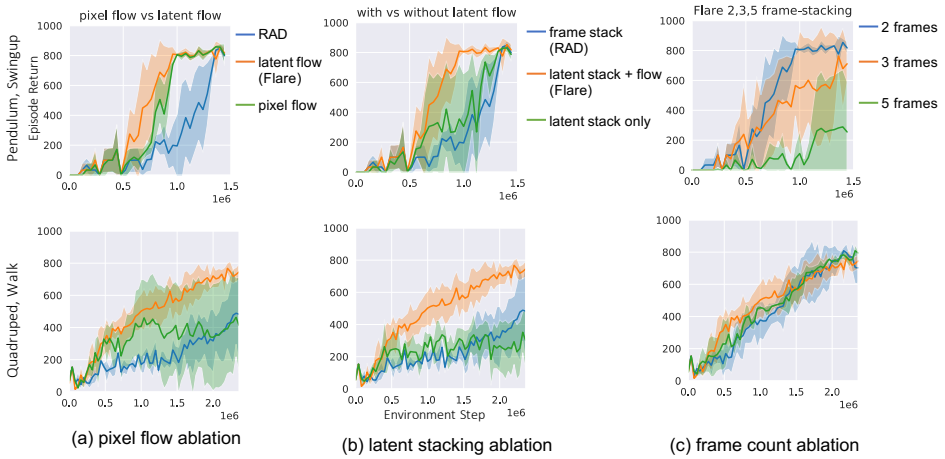

Figure 5: We perform 3 ablation studies: (a) *Pixel flow ablation*: we compare using pixel-level and latent-level (Flare) differences. Flare is more stable and performs better. (b) *Latent stack ablation*: we compare using latent stack with and without the latent flow. The latter performs significantly worse, suggesting that the latent flow is crucial. (c) *Frames count ablation*: we test using different number of frames for Flare.

perform worse than FLARE (see Fig 6), which is in agreement with our findings over the poor performance of RNN on coordinate (i.e. compact) state representations in Section 4.

7 Broader Impacts and Limitations

Conclusion We propose Flare, an architecture for RL that explicitly encode temporal information by computing flow in the latent space. In experiments, we show that in the state space, Flare can recover the optimal performance with only state positions and no access to the state velocities. In the pixel space, Flare improves upon the state-of-the-art model-free RL algorithms on the majority of selected tasks in the DMControl and Atari suites, while matching in the remaining. All code assets used for this project came with MIT licenses. For more details, we refer the reader to the appendix.

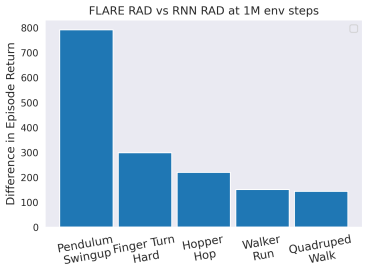

Figure 6: The bars show the difference in episode return between FLARE RAD and RNN at 1M env steps. All experiments are run on a fixed seed. FLARE outperform the RNN baseline in all of the experiments

Limitations Flare is a general approach to improve RL algorithms on many environments and tasks but not the panacea to single-handedly solve all. For instance, learning to control humanoid from pixels remains a challenge even when augmenting RAD with Flare. Also, RAD without Flare in fact is preferred for Seaquest, one of the Atari games. An additional limitation is that Flare is only useful if temporal information such as velocities is visible in the input pixel images and may not work as well for partially observed environments. Finally, Flare was only tested on model-free algorithms and it would be informative to investigate its applicability in the model-based regime, which we leave for future work.

Broader Impacts Simple architectures that improve performance can be impactful due to their ease of use and wide applicability. Prime examples of such innovations in vision are ResNets [18] which have been widely adopted. A potential negative consequence of Flare and supervised RL algorithms in general is that they rely on hand-designed reward functions which can be exploited. For example, in the Quadruped task Flare learns a more optimal policy than prior model-free methods but the resulting policy is extremely jittery since the simulator does not penalize jerk. This policy

would likely wear out the joints if deployed on real robot. To make architectures like Flare and RL in general more applicable to real-world scenarios it would be useful to investigate how to generate safe policies perhaps through constrained optimization or offline RL.

References

[1] Artemij Amiranashvili, Alexey Dosovitskiy, Vladlen Koltun, and Thomas Brox. Motion perception in reinforcement learning with dynamic objects. In *Conference on Robot Learning*, pages 156–168. PMLR, 2018.

[2] Adrià Puigdomènech Badia, Bilal Piot, Steven Kapturowski, Pablo Sprechmann, Alex Vitvitskyi, Daniel Guo, and Charles Blundell. Agent57: Outperforming the atari human benchmark. In *International Conference on Machine Learning*, 2020.

[3] Marc G Bellemare, Yavar Naddaf, Joel Veness, and Michael Bowling. The arcade learning environment: An evaluation platform for general agents. *Journal of Artificial Intelligence Research*, 47:253–279, 2013.

[4] Marc G. Bellemare, Will Dabney, and R. Munos. A distributional perspective on reinforcement learning. In *ICML*, 2017.

[5] Marc G Bellemare, Will Dabney, and Rémi Munos. A distributional perspective on reinforcement learning. *arXiv preprint arXiv:1707.06887*, 2017.

[6] Christopher Berner, Greg Brockman, Brooke Chan, Vicki Cheung, Przemyslaw Debiak, Christy Dennison, David Farhi, Quirin Fischer, Shariq Hashme, Chris Hesse, et al. Dota 2 with large scale deep reinforcement learning. *arXiv preprint arXiv:1912.06680*, 2019.

[7] Joao Carreira and Andrew Zisserman. Quo vadis, action recognition? a new model and the kinetics dataset. In *proceedings of the IEEE Conference on Computer Vision and Pattern Recognition*, pages 6299–6308, 2017.

[8] Yevgen Chebotar, Mrinal Kalakrishnan, Ali Yahya, Adrian Li, S. Schaal, and S. Levine. Path integral guided policy search. *2017 IEEE International Conference on Robotics and Automation (ICRA)*, pages 3381–3388, 2017.

[9] Jeffrey Donahue, Lisa Anne Hendricks, Sergio Guadarrama, Marcus Rohrbach, Subhashini Venugopalan, Kate Saenko, and Trevor Darrell. Long-term recurrent convolutional networks for visual recognition and description. In *Proceedings of the IEEE conference on computer vision and pattern recognition*, pages 2625–2634, 2015.

[10] Alexey Dosovitskiy, German Ros, Felipe Codevilla, Antonio Lopez, and Vladlen Koltun. Carla: An open urban driving simulator. *arXiv preprint arXiv:1711.03938*, 2017.

[11] Lasse Espeholt, Hubert Soyer, Remi Munos, Karen Simonyan, Volodymir Mnih, Tom Ward, Yotam Doron, Vlad Firoiu, Tim Harley, Iain Dunning, et al. Impala: Scalable distributed deep-rl with importance weighted actor-learner architectures. *arXiv preprint arXiv:1802.01561*, 2018.

[12] Christoph Feichtenhofer, Haoqi Fan, Jitendra Malik, and Kaiming He. Slowfast networks for video recognition. In *Proceedings of the IEEE international conference on computer vision*, pages 6202–6211, 2019.

[13] Meire Fortunato, Mohammad Gheshlaghi Azar, Bilal Piot, Jacob Menick, Ian Osband, Alex Graves, Vlad Mnih, Remi Munos, Demis Hassabis, Olivier Pietquin, et al. Noisy networks for exploration. *arXiv preprint arXiv:1706.10295*, 2017.

[14] Tuomas Haarnoja, Aurick Zhou, Pieter Abbeel, and Sergey Levine. Soft actor-critic: Off-policy maximum entropy deep reinforcement learning with a stochastic actor. *arXiv preprint arXiv:1801.01290*, 2018.

[15] Danijar Hafner, Timothy Lillicrap, Jimmy Ba, and Mohammad Norouzi. Dream to control: Learning behaviors by latent imagination. *arXiv preprint arXiv:1912.01603*, 2019.

[16] Danijar Hafner, Timothy Lillicrap, Ian Fischer, Ruben Villegas, David Ha, Honglak Lee, and James Davidson. Learning latent dynamics for planning from pixels. In *International Conference on Machine Learning*, pages 2555–2565. PMLR, 2019.

[17] Hado Hasselt. Double q-learning. *Advances in neural information processing systems*, 23: 2613–2621, 2010.

[18] Kaiming He, Xiangyu Zhang, Shaoqing Ren, and Jian Sun. Deep residual learning for image recognition. In *2016 IEEE Conference on Computer Vision and Pattern Recognition, CVPR 2016, Las Vegas, NV, USA, June 27-30, 2016*, pages 770–778. IEEE Computer Society, 2016. doi: 10.1109/CVPR.2016.90. URL `https://doi.org/10.1109/CVPR.2016.90`.

[19] Matteo Hessel, Joseph Modayil, Hado Van Hasselt, Tom Schaul, Georg Ostrovski, Will Dabney, Dan Horgan, Bilal Piot, Mohammad Azar, and David Silver. Rainbow: Combining improvements in deep reinforcement learning. *arXiv preprint arXiv:1710.02298*, 2017.

[20] Max Jaderberg, Volodymyr Mnih, Wojciech Marian Czarnecki, Tom Schaul, Joel Z Leibo, David Silver, and Koray Kavukcuoglu. Reinforcement learning with unsupervised auxiliary tasks. *arXiv preprint arXiv:1611.05397*, 2016.

[21] Divye Jain, Andrew Li, Shivam Singhal, Aravind Rajeswaran, Vikash Kumar, and Emanuel Todorov. Learning Deep Visuomotor Policies for Dexterous Hand Manipulation. In *International Conference on Robotics and Automation (ICRA)*, 2019.

[22] Shuiwang Ji, Wei Xu, Ming Yang, and Kai Yu. 3d convolutional neural networks for human action recognition. *IEEE transactions on pattern analysis and machine intelligence*, 35(1): 221–231, 2012.

[23] Steven Kapturowski, Georg Ostrovski, John Quan, Remi Munos, and Will Dabney. Recurrent experience replay in distributed reinforcement learning. In *International conference on learning representations*, 2018.

[24] A. Karpathy, G. Toderici, S. Shetty, T. Leung, R. Sukthankar, and L. Fei-Fei. Large-scale video classification with convolutional neural networks. In *2014 IEEE Conference on Computer Vision and Pattern Recognition*, pages 1725–1732, 2014.

[25] Ilya Kostrikov, Denis Yarats, and Rob Fergus. Image augmentation is all you need: Regularizing deep reinforcement learning from pixels. *arXiv preprint arXiv:2004.13649*, 2020.

[26] Michael Laskin, Kimin Lee, Adam Stooke, Lerrel Pinto, Pieter Abbeel, and Aravind Srinivas. Reinforcement learning with augmented data. *arXiv preprint arXiv:2004.14990*, 2020.

[27] Michael* Laskin, Aravind* Srinivas, and Pieter Abbeel. Curl: Contrastive unsupervised representations for reinforcement learning. *Proceedings of the 37th International Conference on Machine Learning, Vienna, Austria, PMLR 119*, 2020. arXiv:2004.04136.

[28] Timothy P. Lillicrap, Jonathan J. Hunt, Alexander Pritzel, Nicolas Heess, Tom Erez, Yuval Tassa, David Silver, and Daan Wierstra. Continuous control with deep reinforcement learning. In *ICLR*, 2016.

[29] Volodymyr Mnih, Koray Kavukcuoglu, David Silver, Andrei A Rusu, Joel Veness, Marc G Bellemare, Alex Graves, Martin Riedmiller, Andreas K Fidjeland, Georg Ostrovski, et al. Human-level control through deep reinforcement learning. *Nature*, 518(7540):529–533, 2015.

[30] Volodymyr Mnih, Adria Puigdomenech Badia, Mehdi Mirza, Alex Graves, Timothy Lillicrap, Tim Harley, David Silver, and Koray Kavukcuoglu. Asynchronous methods for deep reinforcement learning. In *International conference on machine learning*, pages 1928–1937, 2016.

[31] John Quan and Georg Ostrovski. DQN Zoo: Reference implementations of DQN-based agents, 2020. URL `http://github.com/deepmind/dqn_zoo`.

[32] Manolis Savva, Abhishek Kadian, Oleksandr Maksymets, Yili Zhao, Erik Wijmans, Bhavana Jain, Julian Straub, Jia Liu, Vladlen Koltun, Jitendra Malik, et al. Habitat: A platform for embodied ai research. In *Proceedings of the IEEE International Conference on Computer Vision*, pages 9339–9347, 2019.

[33] Tom Schaul, John Quan, Ioannis Antonoglou, and David Silver. Prioritized experience replay. *arXiv preprint arXiv:1511.05952*, 2015.

[34] John Schulman, Filip Wolski, Prafulla Dhariwal, Alec Radford, and Oleg Klimov. Proximal policy optimization algorithms. *arXiv preprint arXiv:1707.06347*, 2017.

[35] Max Schwarzer, Ankesh Anand, Rishab Goel, R Devon Hjelm, Aaron Courville, and Philip Bachman. Data-efficient reinforcement learning with momentum predictive representations. *arXiv preprint arXiv:2007.05929*, 2020.

[36] David Silver, Aja Huang, Christopher J. Maddison, Arthur Guez, Laurent Sifre, George van den Driessche, Julian Schrittwieser, Ioannis Antonoglou, Veda Panneershelvam, Marc Lanctot, Sander Dieleman, Dominik Grewe, John Nham, Nal Kalchbrenner, Ilya Sutskever, Timothy Lillicrap, Madeleine Leach, Koray Kavukcuoglu, Thore Graepel, and Demis Hassabis. Mastering the game of go with deep neural networks and tree search. *Nature*, 529:484–503, 2016. URL `http://www.nature.com/nature/journal/v529/n7587/full/nature16961.html`.

[37] David Silver, Julian Schrittwieser, Karen Simonyan, Ioannis Antonoglou, Aja Huang, Arthur Guez, Thomas Hubert, Lucas Baker, Matthew Lai, Adrian Bolton, Yutian Chen, Timothy Lillicrap, Fan Hui, Laurent Sifre, George Driessche, Thore Graepel, and Demis Hassabis. Mastering the game of go without human knowledge. *Nature*, 550:354–359, 10 2017. doi: 10.1038/nature24270.

[38] Karen Simonyan and Andrew Zisserman. Two-stream convolutional networks for action recognition in videos. In *Advances in neural information processing systems*, pages 568–576, 2014.

[39] Samarth Sinha, Homanga Bharadhwaj, Aravind Srinivas, and Animesh Garg. D2rl: Deep dense architectures in reinforcement learning, 2020.

[40] Khurram Soomro, Amir Roshan Zamir, and Mubarak Shah. Ucf101: A dataset of 101 human actions classes from videos in the wild. *arXiv preprint arXiv:1212.0402*, 2012.

[41] Richard Sutton and Andrew Barto. *Reinforcement Learning: An Introduction*. MIT Press, 1998.

[42] Yuval Tassa, Yotam Doron, Alistair Muldal, Tom Erez, Yazhe Li, Diego de Las Casas, David Budden, Abbas Abdolmaleki, Josh Merel, Andrew Lefrancq, et al. Deepmind control suite. *arXiv preprint arXiv:1801.00690*, 2018.

[43] Emanuel Todorov, Tom Erez, and Yuval Tassa. Mujoco: A physics engine for model-based control. In *IROS*, 2012.

[44] Du Tran, Lubomir Bourdev, Rob Fergus, Lorenzo Torresani, and Manohar Paluri. Learning spatiotemporal features with 3d convolutional networks. In *Proceedings of the IEEE international conference on computer vision*, pages 4489–4497, 2015.

[45] Oriol Vinyals, Igor Babuschkin, Wojciech M. Czarnecki, Michaël Mathieu, Andrew Dudzik, Junyoung Chung, David H. Choi, Richard Powell, Timo Ewalds, Petko Georgiev, Junhyuk Oh, Dan Horgan, Manuel Kroiss, Ivo Danihelka, Aja Huang, Laurent Sifre, Trevor Cai, John P. Agapiou, Max Jaderberg, Alexander S. Vezhnevets, Rémi Leblond, Tobias Pohlen, Valentin Dalibard, David Budden, Yury Sulsky, James Molloy, Tom L. Paine, Caglar Gulcehre, Ziyu Wang, Tobias Pfaff, Yuhuai Wu, Roman Ring, Dani Yogatama, Dario Wünsch, Katrina McKinney, Oliver Smith, Tom Schaul, Timothy Lillicrap, Koray Kavukcuoglu, Demis Hassabis, Chris Apps, and David Silver. Grandmaster level in starcraft ii using multi-agent reinforcement learning. *Nature*, 575(7782):350–354, 2019. doi: 10.1038/s41586-019-1724-z. URL `https://doi.org/10.1038/s41586-019-1724-z`.

[46] Aaron Walsman, Yonatan Bisk, Saadia Gabriel, Dipendra Misra, Yoav Artzi, Yejin Choi, and Dieter Fox. Early Fusion for Goal Directed Robotic Vision. In *International Conference on Intelligent Robots and Systems (IROS)*, 2019.

[47] Xiaolong Wang, Ross Girshick, Abhinav Gupta, and Kaiming He. Non-local neural networks. In *Proceedings of the IEEE conference on computer vision and pattern recognition*, pages 7794–7803, 2018.

[48] Ziyu Wang, Tom Schaul, Matteo Hessel, Hado Hasselt, Marc Lanctot, and Nando Freitas. Dueling network architectures for deep reinforcement learning. In *International conference on machine learning*, pages 1995–2003, 2016.

[49] Ziyu Wang, Alexander Novikov, Konrad Zolna, Jost Tobias Springenberg, Scott Reed, Bobak Shahriari, Noah Siegel, Josh Merel, Caglar Gulcehre, Nicolas Heess, and Nando de Freitas. Critic regularized regression, 2020.

[50] Denis Yarats, Amy Zhang, Ilya Kostrikov, Brandon Amos, Joelle Pineau, and Rob Fergus. Improving sample efficiency in model-free reinforcement learning from images. *arXiv preprint arXiv:1910.01741*, 2019.